*J. Fluid Mech.* (1986), *vol.* 162, *pp.* 99–116
*Printed in Great Britain*



# The evolution of resonant water-wave oscillations

By EDWARD A. COX
Department of Mathematical Physics, University College Dublin, Ireland

AND MICHAEL P. MORTELL
Registrar's Office, University College Cork, Ireland

(Received 25 February 1985)

This paper is concerned with the evolution of small-amplitude, long-wavelength, resonantly forced oscillations of a liquid in a tank of finite length. It is shown that the surface motion is governed by a forced Korteweg–de Vries equation. Numerical integration indicates that the motion does not evolve to a periodic steady state unless there is dissipation in the system. When there is no dissipation there are cycles of growth and decay reminiscent of Fermi–Pasta–Ulam recurrence. The experiments of Chester & Bones (1968) show that for certain frequencies more than one periodic solution is possible. We illustrate the evolution of two such solutions for the fundamental resonance frequency.

## 1. Introduction

This paper is concerned with the evolution of small-amplitude, long-wavelength, forced oscillations of a liquid in a tank of finite length. The liquid is subject to a periodic excitation generated by a piston wavemaker that operates at resonant and near-resonant frequencies. The roles of nonlinearity (amplitude dispersion), frequency dispersion and dissipation in the evolving motion of the liquid are examined. A central issue is the existence of a steady periodic state, and indeed, the existence of more than one such state, for a given frequency.

The study of resonant oscillations in the context of a column of gas in a closed tube began with the experiments of Lettau (1939), which exhibited periodic shocks travelling in the tube, and Betchov (1958) who gave the first theoretical explanation. The latter showed that the amplitude at resonance was finite and determined by amplitude dispersion. Chester (1964) gave a small-rate theory in which the transition from a continuous waveform away from resonance to a waveform containing shocks near resonance arises naturally. A finite-rate theory, which allows distortion of the waveform as it travels in the tube, was given by Seymour & Mortell (1980) who introduced a functional equation, known as the 'standard mapping', which is intimately connected with chaotic motions; see Chirikov (1979), Mortell & Seymour (1980). Using the acoustic analogy, Verhagen & Wijngaarden (1965) treated the time-periodic response of resonantly excited shallow-water waves in a finite-length tank. Chester (1968) gave a theory that included the effects of frequency dispersion and boundary-layer damping in the walls of the tank, and Chester & Bones (1968) gave the confirmation between numerical and experimental results to show the significance of these effects. For wavemaker frequencies in a band about a resonant frequency, waves produced in the tank are characterized by high peaks separated by long troughs, and the amplitude of the response, though small, is of a larger order of magnitude than the wavemaker amplitude. At certain discrete frequencies abrupt

changes in amplitude occur, with a corresponding change in the signal shape. Outside of the resonant band the wave profile is adequately calculated from acoustic theory. These results are confirmed by Ockendon & Ockendon (1973), where an asymptotic analysis is employed to elucidate key features of the solution.

All the papers to which we have referred above are concerned only with the construction of solutions when the induced oscillations have settled down to the final periodic state. The first paper to address the question as to how such periodic oscillations might evolve from a given initial state was that of Cox & Mortell (1983). That paper considered the evolution of resonant oscillations of an inviscid gas in a closed tube from an initial state of rest. It was shown how continuous solutions and solutions containing shocks evolve, and how the details of the initial state are absorbed by shocks as time progresses even in the case when the periodic state is shockless. More recently, Seymour & Mortell (1985) treated the evolution of finite-rate oscillations of a gas in a closed tube by the analysis of a functional equation.

In the present paper an evolution equation – a modified periodically forced Korteweg–de Vries equation – is derived for the resonant forcing of shallow-water waves in a tank, and the predictions are compared with the numerical and experimental results of Chester & Bones (1968). The order of magnitude of the resonant oscillations in the periodic state is larger than that of the forcing amplitude and, hence, of the amplitude of the fluid oscillations in the early stages of the evolution. The evolution equation is then dependent on the amplitude parameter to allow the variation with time of the order of magnitude of the solution amplitude. The predictions of the theory given here are confirmed by experiments. The change in the number of undulations in the waveform with the change in frequency is reproduced, and the non-uniqueness is confirmed by exhibiting the evolution of two distinct solutions at the fundamental resonance.

It is also worthy of note that the numerical results indicate that a dissipative mechanism is essential for a periodic state to be attained. When dissipative effects are excluded from the evolution equation the numerical results indicate a recurrence phenomenon reminiscent of that in Zabusky & Kruskal (1965).

In §2 the waves in the tank are shown to propagate according to acoustic theory, while the signal propagated is determined by a nonlinear functional differential equation. This latter equation is reduced to a partial differential equation in §3 by the use of a two-variable expansion technique. The motion in the tank is thus the superposition of oppositely travelling, non-interacting waves where the signal carried by a wave is determined by a periodically forced Korteweg–de Vries equation. The effect of dissipation is introduced in §5. Numerical solutions are presented in §§4 and 5 and comparison is made with the experimental results, which are mainly available for the periodic motions only.

## 2. Formulation: derivation of functional differential equation

Consider the two-dimensional irrotational motion of an inviscid, incompressible, homogeneous fluid, with density $\rho_0$, subject to a constant gravitational force $g$. The fluid, of undisturbed depth $H$, rests on a horizontal impermeable bed located at $z = -H$ and has a free surface at $z = \eta(x, t)$. The fluid is contained in a tank of finite length $L$, closed at end $x = 0$ and with an idealized wavemaker oscillating with maximum displacement $l$ located at $x = L - l\cos\omega t$.

Waves generated in the fluid are analysed under the following assumptions. We assume that the length of the tank is much larger than the depth of fluid, so that

$$\delta = \frac{H}{L} \ll 1, \tag{2.1}$$

and that the wavemaker amplitude $l$ is small compared to the length of the tank, i.e.

$$\epsilon = \frac{l}{L} \ll 1. \tag{2.2}$$

The behaviour of the fluid is characterized then by the two small dimensionless parameters $\epsilon$ and $\delta$, and approximations developed depend on the relationship assumed between those parameters.

It is convenient to express the fluid flow in the dimensionless variables:

$$\phi' = \frac{\phi}{c_0 L}, \quad t' = \frac{\omega t}{\pi}, \quad \eta' = \frac{\eta}{H}, \quad x' = \frac{x}{L}, \quad p' = \frac{p_0}{\rho_0 c_0}, \quad \omega' = \frac{\omega L}{2\pi c_0},$$

where $\phi$ is the velocity potential, $p_0$ is the pressure at the free surface, $\rho_0$ the fluid density, $\omega$ the frequency of the wavemaker and $c_0 = (gH)^{\frac{1}{2}}$ the long-wave speed.

In dimensionless variables (dropping the primes) the fluid has a velocity potential which satisfies

$$\delta^2 \frac{\partial^2 \phi}{\partial x^2} + \frac{\partial^2 \phi}{\partial z^2} = 0 \quad (0 < x < 1 - \epsilon \cos \pi t, \ -1 < z < \eta(x, t)), \tag{2.3}$$

subject to the boundary conditions on the free surface and on the bottom and ends of the tank. The bottom of the tank is impermeable, so that

$$\frac{\partial \phi}{\partial z} = 0 \quad \text{on } z = -1. \tag{2.4}$$

On the free surface $z = \eta(x, t)$ the dynamic and kinematic conditions imply

$$2\omega \frac{\partial \phi}{\partial t} + \frac{1}{2}\left[\left(\frac{\partial \phi}{\partial x}\right)^2 + \delta^{-2}\left(\frac{\partial \phi}{\partial z}\right)^2\right] + \eta = 0, \tag{2.5}$$

and

$$\frac{\partial \phi}{\partial z} - \delta^2 \left[2\omega \frac{\partial \eta}{\partial t} + \frac{\partial \eta}{\partial x}\frac{\partial \phi}{\partial x}\right] = 0. \tag{2.6}$$

Since the tank is closed at the end $x = 0$, the boundary condition is

$$\frac{\partial \phi}{\partial x}(0, z, t) = 0 \quad (-1 < z < \eta(x, t)). \tag{2.7}$$

The wavemaker imparts a small-amplitude sinusoidal velocity at $x = 1 - \epsilon \cos \pi t$, which implies that

$$u = \frac{\partial \phi}{\partial x}(x, z, t) = 2\pi\epsilon\omega \sin \pi t \quad (-1 < z < \eta(x, t)). \tag{2.8}$$

The initial conditions for the fluid flow defined by (2.3)–(2.8) are those corresponding to an undisturbed fluid, so that

$$\left.\begin{aligned} \eta = \eta_t = 0 \\ \phi_x = 0 \end{aligned}\right\} \text{ for } t \leqslant 0, \ -1 < z < 0, \ 0 \leqslant x \leqslant 1. \tag{2.9}$$

The aim of this section is to derive an asymptotic approximation to (2.3)–(2.9) that will describe the evolution of small-amplitude, large-wavelength oscillations of the fluid when the wavemaker is operating at or near the fundamental resonant frequency $\omega = \frac{1}{2}$. The independent parameters that control the effects of nonlinearity and frequency dispersion are $\epsilon$ and $\delta$ respectively. The theory given in Chester (1968) shows that in the periodic state there is a balance of nonlinearity and frequency dispersion, while Ockendon & Ockendon (1973) give the similarity relation

$$\delta^2 = \kappa\epsilon^{\frac{1}{2}} \tag{2.10}$$

for the periodic motion when the amplitude is $O(\epsilon^{\frac{1}{2}})$. The similarity relationship usually adopted is

$$\delta^2 = \kappa\epsilon, \tag{2.11}$$

see Mortell (1977) or Kevorkian & Cole (1981), but it should be noted that the underlying assumption is that the response amplitude is $O(\epsilon)$. In the case treated here, while the input amplitude is $O(\epsilon)$ the periodic response at resonance is $O(\epsilon^{\frac{1}{2}})$, and hence the relationship as adopted in (2.10) ensures the appropriate balance in the periodic state.

We expand the velocity potential and free-surface shape as follows:

$$\left.\begin{aligned} \phi(x, z, t; \epsilon) &= \epsilon\phi_0(x, z, t) + \epsilon^{\frac{3}{2}}\phi_1(x, z, t) + \epsilon^2\phi_2(x, z, t) + O(\epsilon^{\frac{5}{2}}) \\ \eta(x, t; \epsilon) &= \epsilon\eta_0(x, t) + \epsilon^{\frac{3}{2}}\eta_1(x, t) + \epsilon^2\eta_2(x, t) + O(\epsilon^{\frac{5}{2}}), \end{aligned}\right\} \tag{2.12}$$

and assume that the relationship (2.10) between $\epsilon$ and $\delta$ holds. As we are interested in the response close to the fundamental acoustic resonant frequency $\omega = \frac{1}{2}$, we introduce the detuning parameter $\bar{\Delta}$ by

$$\bar{\Delta} = \epsilon^{\frac{1}{2}}\Delta = 2\omega - 1 \quad (\Delta = O(1)). \tag{2.13}$$

Substitution of (2.10)–(2.12) into equations (2.3) and (2.4) yields

$$\phi_0 = \theta_0(x, t), \tag{2.14}$$

$$\phi_1 = \theta_1(x, t) - \tfrac{1}{2}\kappa(1+z)^2\frac{\partial^2\theta_0}{\partial x^2}, \tag{2.15}$$

$$\phi_2 = \theta_2(x, t) - \tfrac{1}{2}\kappa(1+z)^2\frac{\partial^2\theta_1}{\partial x^2} + \tfrac{1}{24}\kappa^2(1+z)^4\frac{\partial^4\theta_0}{\partial x^4}. \tag{2.16}$$

The free-surface conditions (2.5) and (2.6) then imply

$$\frac{\partial^2\theta_0}{\partial x^2} - \frac{\partial^2\theta_0}{\partial t^2} = 0, \tag{2.17}$$

$$\frac{\partial^2\theta_1}{\partial x^2} - \frac{\partial^2\theta_1}{\partial t^2} = \kappa\left(\frac{1}{6}\frac{\partial^4\theta_0}{\partial x^4} - \frac{1}{2}\frac{\partial^4\theta_0}{\partial x^2\partial t^2}\right) + 2\Delta\frac{\partial^2\theta_0}{\partial x^2}, \tag{2.18}$$

$$\begin{aligned} \frac{\partial^2\theta_2}{\partial x^2} - \frac{\partial^2\theta_2}{\partial t^2} = \kappa\left(\frac{\kappa}{32}\frac{\partial^6\theta_0}{\partial x^4\partial t^2} - \frac{1}{3}\frac{\partial^4\theta_1}{\partial x^4}\right) + 2\Delta\left(\frac{\partial^2\theta_1}{\partial t^2} + \frac{\partial^4\theta_0}{\partial x^2\partial t^2} + \tfrac{1}{2}\Delta\frac{\partial^2\theta_0}{\partial t^2}\right) \\ + 2\frac{\partial\theta_0}{\partial x}\frac{\partial^2\theta_0}{\partial x\partial t} + \frac{\partial\theta_0}{\partial t}\frac{\partial^2\theta_0}{\partial x\partial t}, \end{aligned} \tag{2.19}$$

where $\eta_0$, $\eta_1$, $\eta_2$ are eliminated. The condition (2.8) corresponding to an idealized wavemaker on the moving boundary $x = 1-\epsilon\cos\pi t$ gives

$$\frac{\partial\phi_0}{\partial x} = \pi\sin\pi t, \tag{2.20}$$

$$\frac{\partial\phi_1}{\partial x} = \Delta\pi\sin\pi t, \tag{2.21}$$

$$\frac{\partial\phi_2}{\partial x} = \frac{\partial^2\phi_0}{\partial x^2}\cos\pi t, \tag{2.22}$$

on the fixed boundary $x = 1$.

The linear, non-dispersive approximation is given by (2.17), which gives the result

$$\phi_0 = \theta_0(x, t) = f(t+x-1)+g(t-x), \tag{2.23}$$

where $f$ and $g$ are arbitrary functions. The boundary conditions (2.7) on $x = 0$ and (2.20) on $x = 1$ imply

$$h(t)-h(t-2) = \pi\sin\pi t, \tag{2.24}$$

where $h(t) = f'(t)$ and $f'(t-1) = g'(t)$. The initial condition corresponding to (2.9) is

$$h(t) = 0 \quad (t \leqslant 0). \tag{2.25}$$

For $t > 0$, (2.24) yields

$$h(t) = \tfrac{1}{2}\pi t\sin\pi t, \tag{2.26}$$

which shows the linear growth associated with an acoustic theory of resonance.

We shall continue to adopt the acoustic representation (2.23) for the propagation of the oscillations, without distortion, in the fluid, and then operate within the small-rate limit; see Seymour & Mortell (1980). However, we must go beyond the acoustic approximation and include terms corresponding to amplitude and frequency dispersion in deriving an equation to determine the evolution of the propagating signal. The necessity for the different levels of approximation to determine the mode of propagation and the signal propagated is recognized in the papers by Chester (1964, 1968), Seymour & Mortell (1973, 1980) and Cox & Mortell (1983).

On substituting for $\theta_0$ from (2.23) into (2.18), we obtain the particular integral for $\partial\theta_1/\partial x$ as

$$\frac{\partial\theta_1}{\partial x} = \tfrac{1}{12}\kappa(g'''(t-x)-f'''(t+x-1)-\tfrac{1}{6}\kappa x(f^{\mathrm{iv}}(t+x-1)+g^{\mathrm{iv}}(t-x)) \\ +\tfrac{1}{2}\Delta(f'(t+x-1)-g'(t-x))+\Delta x(g''(t-x)+f''(t+x-1)), \tag{2.27}$$

and the complementary functions are absorbed into the presentation (2.23) for $\theta_0$.

It should be noted here that the terms in (2.27) are essentially due to the frequency dispersion, since $\Delta$ may be set equal to zero at resonance. Thus the form of the expansions assumed in (2.11) and (2.12) brings in the frequency dispersion terms at $O(\epsilon^{\frac{3}{2}})$, prior to the nonlinear terms at $O(\epsilon^2)$. The particular integral for $\partial\theta_2/\partial x$ corresponding to the nonlinear terms in (2.19) is

$$\frac{\partial\theta_2}{\partial x} = \tfrac{3}{2}x[g'(t-x)\,g''(t-x)+f'(t+x-1)f''(t+x-1)]+\tfrac{3}{2}[\{f'(t+x-1)\}^2-\{g'(t-x)\}^2] \\ +[f(t+x-1)\,g''(t-x)-g(t-x)f''(t+x-1)]. \tag{2.28}$$

The representation for $u = \partial\phi/\partial x$, from which the evolution equation for $h(t) = f'(t)$ on the boundary $x = 1$ will be derived, is

$$\frac{\partial\phi}{\partial x} = \epsilon\frac{\partial\theta_0}{\partial x} + \epsilon^{\frac{3}{2}}\frac{\partial\theta_1}{\partial x} + \epsilon^2\frac{\partial\theta_2}{\partial x}, \tag{2.29}$$

where $\theta_0$, $\theta_1$ and $\theta_2$ are given by (2.23), (2.27) and (2.28) respectively. The terms neglected in (2.28) are linear functions of derivatives of $f$ and $g$ and will remain bounded if $f$ and $g$ are bounded and, furthermore, correspond to no new physical effect. Applying the boundary condition (2.7) at $x = 0$ to the representation (2.29) yields the relation

$$g'(t) = f'(t-1). \tag{2.30}$$

Then the combination of the boundary conditions (2.20) and (2.21) on $x = 1$ applied to the expression (2.29), and noting the relation (2.30), implies

$$\begin{aligned}2\pi\omega\sin\pi t = {} & h(t)-h(t-2)\\ & +\epsilon^{\frac{1}{2}}[\tfrac{1}{12}\kappa\{h''(t-2)-h''(t)\}-\tfrac{1}{6}\kappa(h'''(t-2)+h'''(t)\}\\ & \qquad +\tfrac{1}{2}\Delta\{h(t)-h(t-2)\}+\Delta\{h'(t-2)+h'(t)\}]\\ & +\epsilon\Big[\tfrac{3}{2}\{h(t)\,h'(t)+h(t-2)\,h'(t-2)+h^2(t)-h^2(t-2)\}\\ & \qquad +h'(t-2)\int^t h(s)\,\mathrm{d}s - h'(t)\int^{t-2} h(s)\,\mathrm{d}s\Big],\end{aligned} \tag{2.31}$$

where $h(t) = f'(t)$. The boundary condition (2.22) has not been used since it is a correction term both at the initial stages of the motion when the velocity $u = O(\epsilon)$, and at the final stage when $u = O(\epsilon^{\frac{1}{2}})$.

Equation (2.31), which determines the function $h(t)$ and hence the first approximation to the fluid velocity and free-surface displacement, is a nonlinear differential-difference equation. The terms on the right-hand side of (2.31) that are independent of $\epsilon$ are those corresponding to acoustic theory, the $\kappa\epsilon^{\frac{1}{2}}$ terms are those corresponding to frequency dispersion, while the $\epsilon$ terms correspond to nonlinearity (amplitude dispersion) and the nonlinear interaction of oppositely travelling waves. In the early stages of the motion the amplitude is $O(\epsilon)$ and the acoustic terms are dominant. This results in linear growth of the amplitude until at $O(\epsilon^{\frac{1}{2}})$ the frequency dispersion become effective and eventually strikes a balance with the steepening effects of the nonlinearity.

The ordinary differential equation governing the periodic motion is easily derived from (2.31) by seeking a solution with a period equal to that of the driver. Thus we obtain

$$\tfrac{3}{2}RR' + \Delta R' - \tfrac{1}{6}\kappa R''' = \pi\omega\sin\pi t, \tag{2.32}$$

where

$$R(t) = \epsilon^{\frac{1}{2}}h(t). \tag{2.33}$$

Equation (2.32) is essentially the result given by Ockendon & Ockendon (1973).

## 3. Governing partial differential equation

The functional differential equation (2.31) was derived in the previous section by incorporating into the basic approximation those terms which represent the pertinent physical effects. In this section we show how (2.31) can be reduced to a nonlinear

partial differential equation by the application of a two-variable expansion technique. Mortell (1977) and Kevorkian & Cole (1981) showed that, using appropriate variables, standing waves on shallow water confined to a tank of finite length satisfied a Korteweg–de Vries equation, which described the evolution of the signal on the boundaries. With the introduction of two timescales, we show here that the evolution of the signal on the boundary $x = 1$ is described by a periodically forced Korteweg–de Vries equation.

There are two natural timescales associated with this problem – the scale identified by the variable $t^+ = t$, which is a measure of the time for a signal to travel the length of the tank, and the scale $\tau = \epsilon t^+$, which measures the time over which nonlinear effects became significant. The validity of the following technique requires that the latter scale is much larger than the former. This is a small-rate assumption. We assume expansions of the form

$$h(t;\epsilon) = h_0(t^+, \tau) + \epsilon h_1(t^+, \tau) + \ldots, \tag{3.1}$$

and also note that

$$h(t-2;\epsilon) = h_0(t^+-2, \tau) - 2\epsilon \frac{\partial h_0}{\partial \tau}(t^+-2, \tau) + \epsilon h_1(t^+-2, \tau) + \ldots. \tag{3.2}$$

Solutions of (2.31) are sought which are periodic in the fast-time variable $t^+$ with the same period as the wavemaker and are slowly modulated on the long timescale $\tau$. Thus we assume that

$$h_i(t^+-2, \tau) = h_i(t^+, \tau) \quad (i = 0, 1, 2, \ldots). \tag{3.3}$$

The functional differential equation (2.31) then reduces to

$$\epsilon \frac{\partial h_0}{\partial \tau} + \epsilon \tfrac{3}{2} h_0 \frac{\partial h_0}{\partial t^+} + \bar{\Delta} \frac{\partial h_0}{\partial t^+} - \frac{\delta^2}{6} \frac{\partial^3 h_0}{\partial t^{+3}} = \pi\omega \sin \pi t^+, \tag{3.4}$$

with

$$h_0(t^+-2, \tau) = h_0(t^+, \tau), \tag{3.5}$$

on substituting (3.1), (3.2) into (2.31) and using (3.3), where terms of $O(\epsilon^{\frac{3}{2}})$ have been neglected. The physical parameters $\delta$, $\epsilon$, and $\bar{\Delta}$ in (3.4) are given by (2.1), (2.2) and (2.13) respectively. It is interesting to note that, as in the standing-wave case, oppositely travelling waves do not interact to this order of approximation. The appropriate initial condition for (3.4) is derived from (2.9) as

$$h_0(t^+, 0) \equiv 0, \tag{3.6}$$

and corresponds to the fluid in a state of rest. Since the solution of (3.4) is periodic in $t^+$ with period 2, integration over one period yields the mean condition

$$\int_0^2 h_0(s, \tau)\, \mathrm{d}s = 0. \tag{3.7}$$

This must not be interpreted as imposing a mean on the physical solution. The physical solution to (3.4) associated with (2.31) requires that $h_0(t^+, \tau)$ be evaluated along the line $\tau = \epsilon t^+$, $t^+ \geqslant 0$, whereas the mean condition (3.7) refers to $h_0(t^+, \tau)$ evaluated on lines of constant $\tau$.

Equation (3.4) is a periodically forced Korteweg–de Vries equation with the periodic boundary condition (3.5). According to acoustic theory, when $t = O(\epsilon^{-\frac{1}{2}})$, $h_0 = O(\epsilon^{-\frac{1}{2}})$ (3.4) becomes

$$\frac{\partial R}{\partial \bar{\tau}} + \tfrac{3}{2} R \frac{\partial R}{\partial t^+} + \Delta \frac{\partial R}{\partial t^+} - \tfrac{1}{6}\kappa \frac{\partial^3 R}{\partial t^{+3}} = \pi\omega \sin \pi t^+, \tag{3.8}$$

where $\bar{\tau} = \epsilon^{\frac{1}{2}}t^+$ and $R = \epsilon^{\frac{1}{2}}h_0$. Equation (3.8) describes the evolution of the signal in the long time and may be derived by a standard perturbation expansion in powers of $\epsilon^{\frac{1}{2}}$, which is the amplitude of the periodic motion. Such a derivation was presented by Jones & Hulme (1983) at the British Theoretical Mechanics Colloquium. The standing-wave result given by Mortell (1977) is recovered from (3.8) by setting the forcing term to zero and taking $\Delta = 0$.

If one considers the periodic motion which is independent of $\bar{\tau}$ then (3.8) reduces to

$$\tfrac{3}{2}R\frac{\mathrm{d}R}{\mathrm{d}t^+} + \Delta\frac{\mathrm{d}R}{\mathrm{d}t^+} - \tfrac{1}{6}\kappa\frac{\mathrm{d}^3R}{\mathrm{d}t^{+3}} = \pi\omega\sin\pi t. \tag{3.9}$$

Equation (3.9) is identical with (2.32), which represents the long-time-periodic solution to the functional differential equation and is equivalent to that obtained by Chester (1968) when appropriate scalings are introduced and dispersion effects are modelled by a differential, rather than an integral, formulation. Equation (3.4), with the periodicity condition (3.5) and initial condition (3.6), represents the evolution of the signal $h_0$ on the boundary $x = 1$. The velocity of the wave motion at any point in the tank is still determined by the linear relation

$$\frac{\partial\phi_0}{\partial x} = h_0(t^+ + x - 1, \tau) - h_0(t^+ - x - 1, \tau), \tag{3.10}$$

while the signal profile is provided by the nonlinear equation (3.4).

## 4. Solutions of forced Korteweg–de Vries equation

This section presents numerical solutions of the periodically forced Korteweg–de Vries equation (3.4). The most comprehensive experimental and numerical results available are those presented by Chester & Bones (1968) for the steady-state periodic problem of 'sloshing' of fluid in a tank. To present results which may be compared directly with those of Chester & Bones we adjust the forcing term in (3.4) to include the effect of an additional sinusoidal-wave generator at $x = 0$. In the present context this is equivalent to replacing boundary condition (2.8) by

$$u = 2\pi\epsilon\omega(1 - \cos 2\pi\omega)\sin\pi t \tag{4.1}$$

on $x = 1 - \epsilon\cos\pi t$. On using (2.5), (2.13) and (2.23) we note that, near resonance, the free surface at $x = 0$ is given by

$$\eta_0|_{x=0} = -2h_0(t^+ - 1, \tau). \tag{4.2}$$

With the substitution $h_0(t^+, \tau) = -f_0(t^+ + 1, \tau)$ (3.4) becomes

$$\epsilon\frac{\partial f_0}{\partial\tau} - \epsilon\tfrac{3}{2}f_0\frac{\partial f_0}{\partial t^+} + \Delta\frac{\partial f_0}{\partial t^+} - \frac{\delta^2}{6}\frac{\partial^3 f_0}{\partial t^{+3}} = \pi\omega(1 - \cos 2\pi\omega)\sin\pi t^+, \tag{4.3}$$

where

$$f_0(t^+ - 2, \tau) = f_0(t^+, \tau). \tag{4.4}$$

The corresponding initial condition is then

$$f_0(t^+, 0) \equiv 0. \tag{4.5}$$

Now $f_0(t^+, \tau)$ can be compared directly with the computed solution profile in Chester & Bones. The steady-state equation derived from (4.3) corresponds to that derived by Chester (1968) under appropriate scaling when the integral representation for

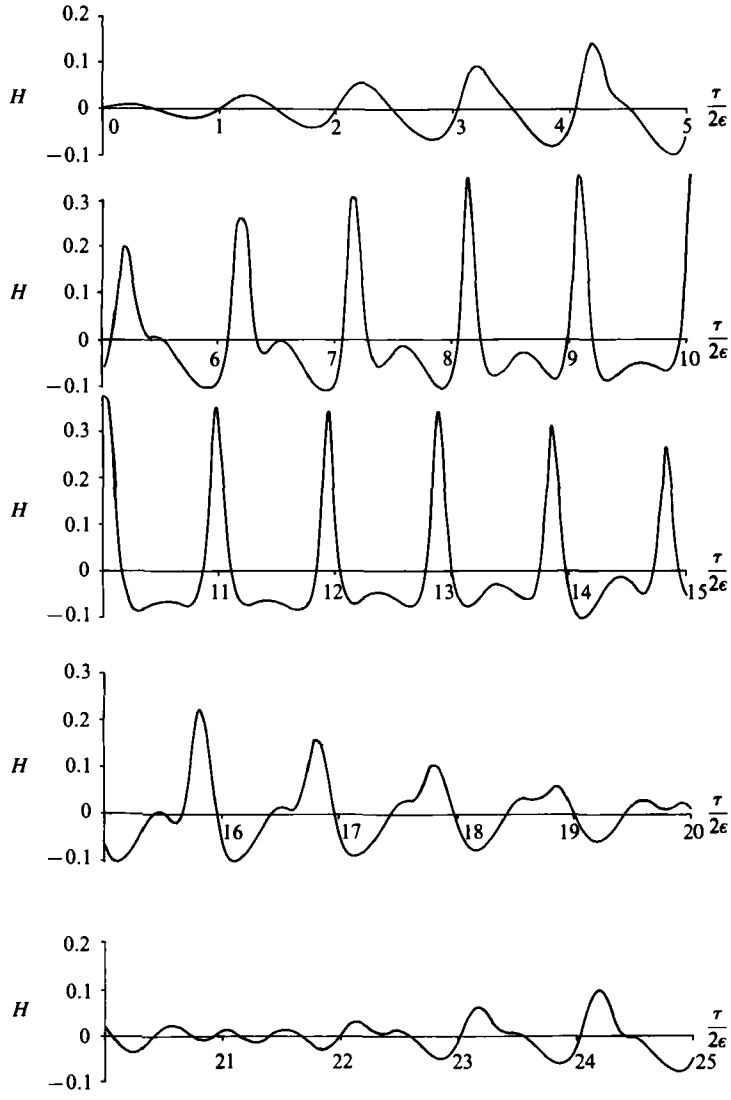


FIGURE 1. Evolution of the signal $H = 3\epsilon\omega f$: no damping. Time $\tau$ is measured in cycles of the wavemaker. $\omega = 0.5$, $\epsilon = 0.00258$, $\delta = 0.083$.

frequency dispersion is replaced by a derivative representation. Additional terms inserted by Chester to extend the validity of his result to regions where linear theory is valid and to take account of damping in the system are ignored in (4.3). As already discussed in §3, to relate (4.3) to the physical problem it is necessary to evaluate $f_0(t^+, \tau)$ along the line $\tau = \epsilon t^+$. The function $f_0(t^+, \tau)$ need only be evaluated for $0 \leqslant t^+ \leqslant 2$, as then the periodicity condition (4.4) enables $f_0$ to be calculated for any value of $t^+$. We evaluate $f_0(t^+, \tau)$ along the lines

$$\tau = \epsilon t^+ + 2\epsilon(n-1), \quad n = 1, 2, 3, \ldots \quad (0 \leqslant t^+ \leqslant 2), \tag{4.6}$$

where $n$ is the number of cycles of the wavemaker after start-up. It should be emphasized that spurious discontinuities arise if $f_0$ is instead constructed from lines of constant $\tau$.

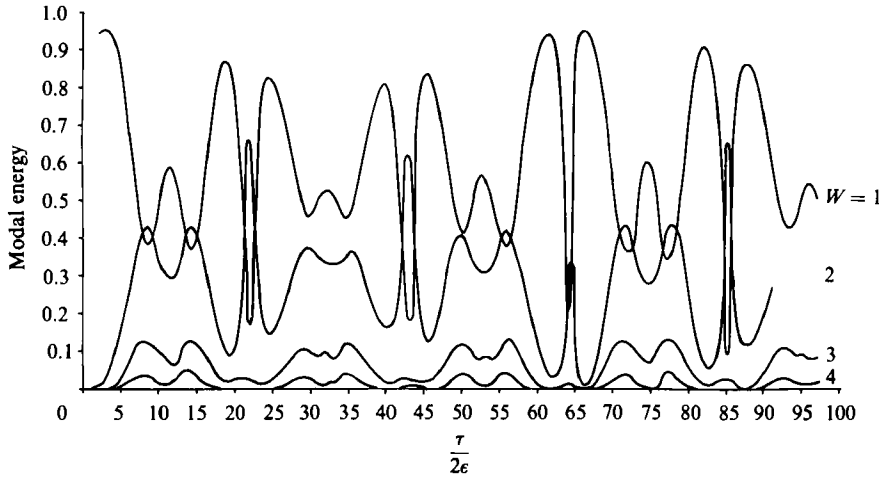


FIGURE 2. Modal energy normalized against the total energy for the modes with wavenumber $W = 1$–4. Generated harmonics are phase-locked to forcing mode $W = 1$: no damping. $\omega = 0.5$, $\epsilon = 0.00258$, $\delta = 0.083$.

Details of the numerical scheme employed to solve (4.3), (4.4) and (4.6) are given in the Appendix. The evolution of the signal is displayed in figure 1 for the first 25 cycles of the wavemaker operating at the resonant frequency $\omega = \frac{1}{2}$ ($\Delta = 0$) for $\epsilon = 0.00258$ and $\delta = 0.083$. We note the initial linear growth in the signal as a prelude to nonlinear effects becoming important. The signal exhibits amplitude growth followed by decay, until in cycle 22 the second harmonic is dominant. This pattern of growth and decay of the signal is repeated. In cycle 66 the signal evolves to approximate the initial behaviour before undergoing a further cycle of growth and decay. The evolution of the energy content of the first four Fourier modes is presented in figure 2, where the total energy in each cycle of the signal is used to normalize the results displayed. Note that second-mode dominance recurs in cycles 43, 64 and 85. We also note that the higher harmonics generated in the signal are phase-locked to the fundamental mode, which is the mode associated with the physical forcing of the system. There is no indication from the numerical results that the signal settles down to a periodic steady state, at least over physically reasonable timescales. A graph of the variation of total energy per cycle with time shows growth and decay in periods of approximately 21 cycles with almost complete return to the initial energy state. Figure 2 provides numerical evidence for the instability, recognized as Fermi–Pasta–Ulam recurrence, of the nonlinear equation (4.3). In the study of oscillations of an anharmonic lattice, Fermi, Pasta & Ulam (1955) reported the repeated return of the energy of the system to approximately the initial state. In the context of deep-water gravity waves Yuen & Ferguson (1978*a*, *b*) have also demonstrated recurrence effects similar to that indicated in figure 2 for a nonlinear Schrödinger equation.

The experiments of Chester & Bones (1968) indicate the existence of periodic steady-state solutions. The theoretical model derived by Chester (1968), and from which his numerical results are calculated, includes the effect of boundary-layer damping in the walls of the tank, and periodic solutions are presented. It will be shown in the next section that the incorporation of damping into the system ensures the existence of a periodic state. In §5 a model for the physical system, which includes damping, is presented together with the numerical results.

## 5. Forced Korteweg–de Vries equation with damping

The numerical results presented in §4 indicate that in the absence of damping the signal profile fails to settle to a steady periodic state. In this section a mathematical model of the physical system, which includes damping, is presented and numerical solutions are given.

Chester (1968) and Ockendon & Ockendon (1973) introduce damping into the system through dissipation, which occurs in the boundary layer on the walls and on the base of the tank. Miles (1976), in examining one-dimensional gravity waves in a viscous fluid, used the same mechanism. Following the method presented in §§2 and 3, inclusion of boundary-layer damping, as discussed in Chester (1968), results in the equation

$$\epsilon\frac{\partial f_0}{\partial\tau}-\frac{\delta^2}{6}\frac{\partial^3 f_0}{\partial t^{+3}}+\bar{\Delta}\frac{\partial f_0}{\partial t^+}-\epsilon\tfrac{3}{2}f_0\frac{\partial f_0}{\partial t^+}+\tfrac{1}{4}\beta\left\{\int_{-\infty}^{\infty}(\operatorname{sgn}(r)+1)\frac{\partial f_0}{\partial t^+}(t^+-r,\tau)\,|\pi r|^{-\frac{1}{2}}\,\mathrm{d}r\right\}$$
$$=\pi\omega(1-\cos 2\pi\omega)\sin\pi t^+, \quad (5.1)$$

which replaces (4.3) as the equation governing the evolution of $f_0$ on $x=1$. The non-dimensional constant $\beta$ is given by

$$\beta=\left\{\frac{L}{h}+\frac{2L}{b}\right\}\bar{\nu}^{\frac{1}{2}}, \quad (5.2)$$

where $b$ is the width of the tank and $\bar{\nu}(=\nu/Lc_0)$ is the non-dimensional coefficient of kinematic viscosity.

Numerical results are presented in figures 3 and 4 for the fundamental frequency $\omega=\frac{1}{2}$ ($\Delta=0$) and with the same physical parameters as in figures 1 and 2. Boundary-layer damping is included through the convolution integral in (5.1) with $\beta=0.0287$. Figure 3 displays the profile of the evolving signal and highlights a period of initial linear growth and development of high peaks separated by a long trough in each period of the wavemaker. Now that damping is included, the numerical results indicate that a steady-state response is attained, and cycle 120, which approximates the periodic state, is displayed. Figure 4 represents the energy content of the first four Fourier modes that constitute the signal, and reveals the effect of boundary-layer damping. It is apparent that, after about 70 cycles of the piston, energy fluctuations are small. A plot of the total energy per cycle in the signal shows the evolution, through a process of damped oscillations, to a constant characterizing the steady-state response.

Details of the numerical scheme employed to solve (5.1) are included in the Appendix. The presence of the convolution integral in (5.1) makes the numerical scheme 'expensive'. A simpler equation, which does not suffer from this disadvantage, and yet for small damping maintains the same solution structure as (5.1), is

$$\epsilon\frac{\partial f_0}{\partial\tau}-\frac{\delta^2}{6}\frac{\partial^3 f_0}{\partial t^{+3}}+\bar{\Delta}\frac{\partial f_0}{\partial t^+}-\epsilon\tfrac{3}{2}f_0\frac{\partial f_0}{\partial t^+}+\lambda f_0=\pi\omega(1-\cos 2\pi\omega)\sin\pi t^+, \quad (5.3)$$

where $\lambda\ll 1$.

The damping introduced in (5.3) is found in a variety of physical situations. It is the form of damping discussed by Ott & Sudan (1970) for ion-sound waves damped by ion–neutral collisions, and by Seymour & Mortell (1973) for energy radiation through one end of a closed tube and for rate dependence of a gas, in the high-frequency limit, in a closed tube. It is expected that, for small values of damping, the structure

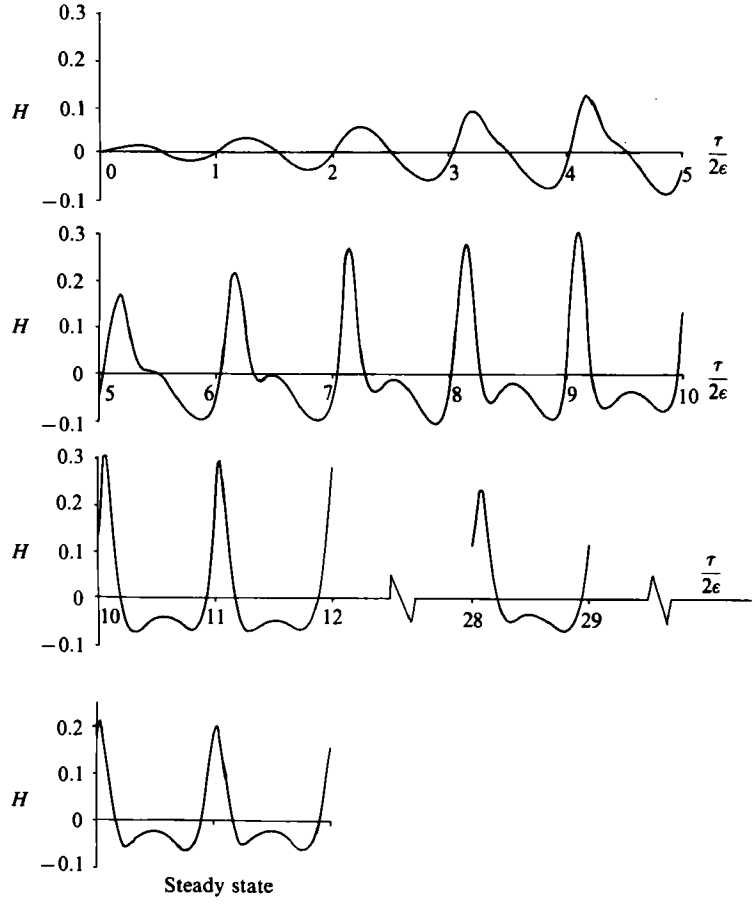


FIGURE 3. Evolution of the signal $H = 3\epsilon\omega f$: boundary-layer damping. $\omega = 0.5$, $\epsilon = 0.00258$, $\delta = 0.083$, $\beta = 0.0287$.

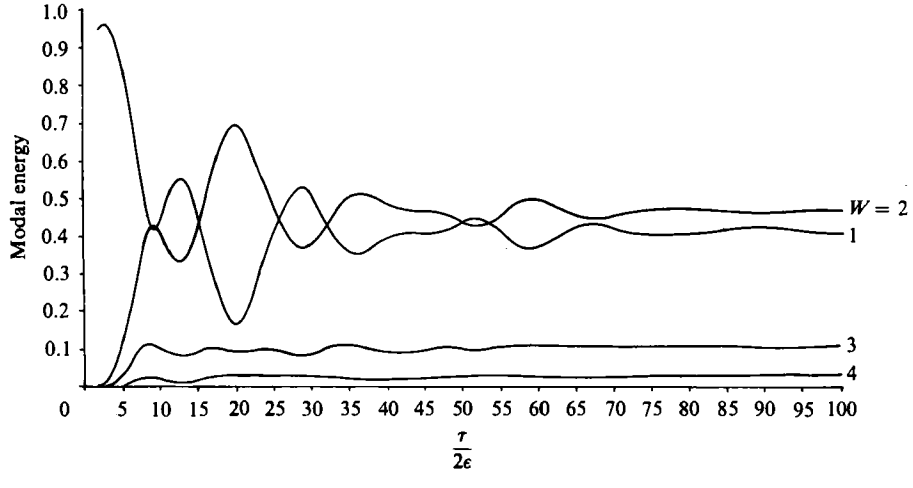


FIGURE 4. Modal energy normalized against the total energy for the modes with wavenumber $W = 1$–$4$: boundary-layer damping. $\omega = 0.5$, $\epsilon = 0.00258$, $\delta = 0.083$, $\beta = 0.0287$.

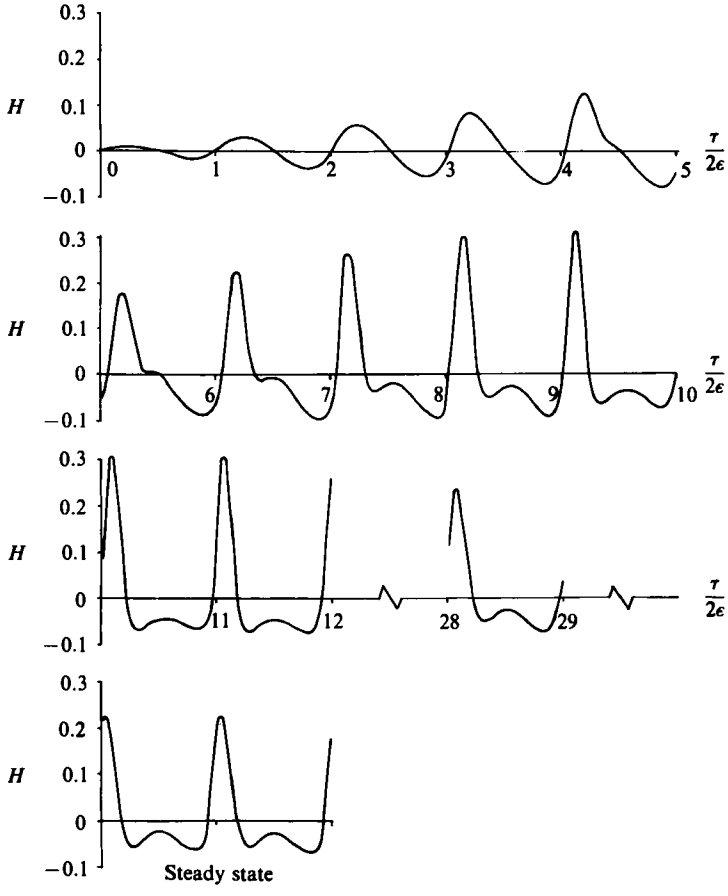


FIGURE 5. Evolution of the signal $H = 3\epsilon\omega f$: damping included. $\omega = 0.5$, $\epsilon = 0.00258$, $\delta = 0.083$, $\lambda = 0.025$.

of the signal will remain insensitive to the precise nature of the damping. This is confirmed by the signal trace displayed in figure 5 for (5.3) for $\omega = \frac{1}{2}$ ($\Delta = 0$), which is in substantial agreement with that in figure 3 when $\lambda = 0.025$. Comparison of numerical solutions of (5.1) and (5.3) for the frequency $\omega = 0.52$ with $\beta = 0.0287$ and $\lambda = 0.025$, and for $\omega = 0.48$ with the same values of $\beta$ and $\lambda$, again give substantial agreement. In these latter-four cases a periodic wave profile is approximately attained in 120 cycles of the wavemaker. It is noted that the structure of the evolving signals corresponding to the given values of $\beta$ and $\lambda$ are quite similar for the three frequencies (no attempt is made to find the best match of $\beta$ and $\lambda$) and the steady-state solutions are in good agreement. On the basis of these results we will adopt (5.3) for the further investigation of the effect of dissipation on the system.

The numerical results for the evolution problem agree well with the periodic results given by Chester (1968). For $\omega = 0.52$ ($r = 0.5$ in Chester's notation) a single peak is quickly established and is maintained in the periodic state; when $\omega = 0.48$ ($r = -0.5$) two peaks per cycle are established, and for $\omega = 0.46$ ($r = -1.2$) three peaks are established. Figure 6 corresponds to the case $\omega = 0.43$ ($r = -2.0$), which lies outside the resonant band. The effects of nonlinearity and frequency dispersion are evident in the evolving signal, which eventually settles down to a periodic form well approximated by acoustic theory. When $\omega = 0.59$ ($r = 2.0$), outside the resonant

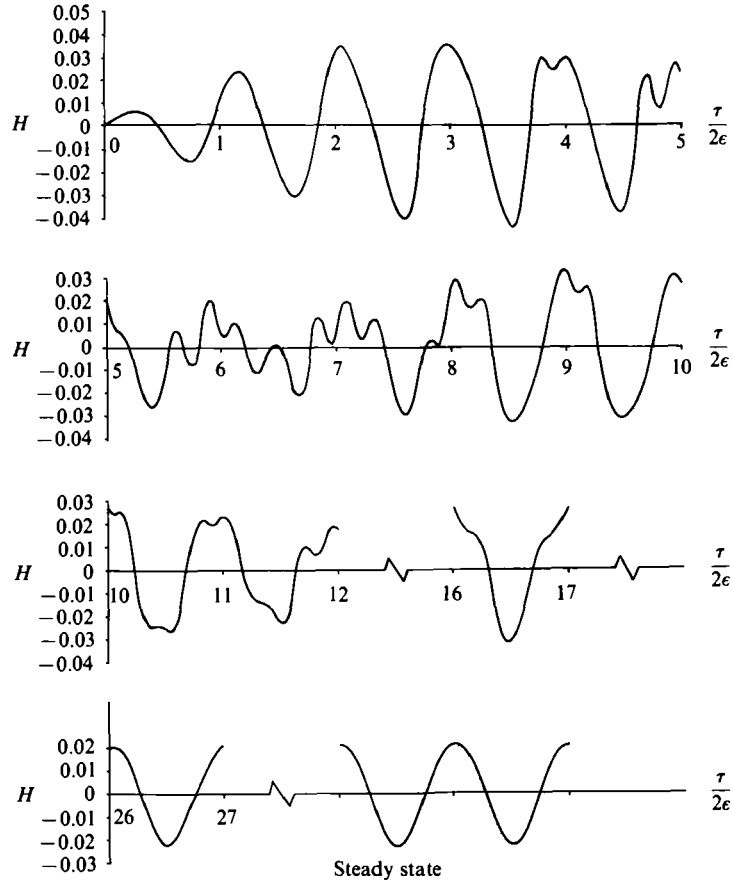


FIGURE 6. Evolution of the signal $H = 3\epsilon\omega f$: damping included. Outside resonant band. $\omega = 0.43$, $\epsilon = 0.00258$, $\delta = 0.083$, $\lambda = 0.025$.

band, there is a beating oscillation which settles down to a periodic form which corresponds to acoustic theory.

The results given above agree with those given in figure 15 of Chester & Bones in that the number of peaks decreases from three to one as the frequency ranges from $\omega = 0.46$ to 0.52.

Chester & Bones (1968) display 'response curves', which bend over near a local maximum, analogous to a hard-spring solution of Duffings' equation. This implies that periodic solutions of the steady-state equations are not unique, and indeed different periodic solutions for the same frequency are displayed. For example, for $\omega = 0.5$ ($r = 0$) in their figure 8 two theoretical solutions are displayed, one containing a single peak per period and one containing two peaks per period. Their figure 18 indicates that two periodic solutions were also found experimentally for $\omega = 0.5$ and figure 11 displays two experimental solutions for $r = 1.06$.

The examples given above concern the evolution of periodic solutions from an initial state of rest and correspond to solutions on the lower branches of the response curves. We wished to produce a periodic solution for the fundamental resonance $\omega = 0.5$, which corresponds to the *upper* branch of the response curve, by using the evolution equation (5.3). A frequency $\omega = 0.48$ was chosen for which the response diagram indicated a unique periodic state, and the solution of (5.3) was allowed to

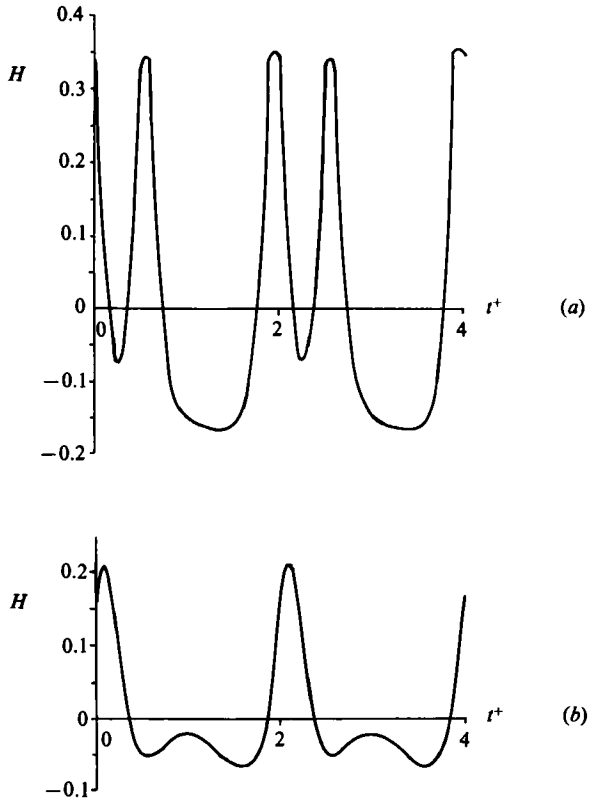


FIGURE 7. Two possible steady-state-signal profiles of $H = 3\epsilon\omega f$. (*a*) corresponds to upper branch of response curve; (*b*) corresponds to lower branch. $\omega = 0.5$, $\epsilon = 0.00258$, $\delta = 0.083$, $\lambda = 0.025$.

evolve for increasing $\tau$. The applied frequency was increased by small amounts until $\omega = 0.5$ in the overlap domain was reached. At each frequency increase the signal was allowed to evolve for some time. Figure 7(*a*) records the steady-state solution for $\omega = 0.5$ obtained in this way, and it can be seen that it contains two peaks per period, in contrast to the lower-branch solution, figure 7(*b*), which has a single peak per period. Thus periodic solutions of the nonlinear, dispersive equation (5.3) are dependent on the initial state, in contrast to periodic solutions of the corresponding nonlinear hyperbolic equation given in Cox & Mortell (1983) where shocks play the vital role of ensuring uniqueness.

As a final example of the theory, we examine the 'beat' oscillation observed experimentally and depicted in their figure 19 by Chester & Bones (1968), which has a period 18 times longer than the period of the forcing term. This 'beat' phenomenon can now be interpreted in terms of Fermi–Pasta–Ulam recurrence cycles as shown in figure 2, and the damping of these cycles as displayed in figure 4. For the physical conditions corresponding to figure 3 there is a 'beat' period of 21 cycles. As figure 4 indicates, the signal evolves through a series of such cycles to the steady state recorded in figure 3. A period of 18 cycles was, however, recorded for the increased forcing amplitude $\epsilon = 0.00516$ corresponding to figure 19 of Chester & Bones (1968) but computing expense prevented tracing the evolution to a steady state. Figure 8 is a typical beat cycle for this forcing amplitude.

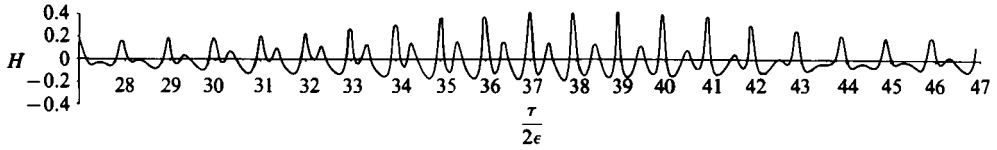


FIGURE 8. Evolution of the signal $H = 3\epsilon\omega f$ over 18 cycles: damping included. Cycles 28–47. $\omega = 0.5$, $\epsilon = 0.00516$, $\delta = 0.083$, $\lambda = 0.025$.

## Appendix

The numerical scheme employed to solve (4.3), (5.1) and (5.3) was proposed by Fornberg (1975) and applied later by Fornberg & Whitham (1978) to the numerical study of the Korteweg–de Vries and related equations. The scheme is a particular example of a pseudospectral method (Kreiss & Oliger 1972) in which the $t^+$ derivatives are approximated by transforming $f_0$ to the discrete Fourier space, where the derivatives are then algebraic quantities, and then transforming back to physical space. A leapfrog (central-difference) scheme advances the solution in $\tau$.

Consider the $t^+$ interval $[0, 2]$. Over this interval we form a uniform mesh of $N = 2M$ points with spaces $\Delta t^+ = 2/2M$. The function $f(t^+, \tau)$ defined at these points is transformed into discrete Fourier space by

$$\hat{f}(W, \tau) = F\{f_0\} = \sum_{j=0}^{2M-1} f_0(j\,\Delta t^+, \tau)\,\mathrm{e}^{-2\pi \mathrm{i} W j/2M}, \quad W = 0, \pm 1, \pm 2, \ldots, \pm M. \tag{A 1}$$

The transformation back to physical space is accomplished by the inversion formula

$$f_0(j\,\Delta t^+, \tau) = F^{-1}\{\hat{f}\} = \frac{1}{N} \sum_{W=-M}^{M} \hat{f}(W, \tau)\,\mathrm{e}^{2\pi \mathrm{i} W j/2M} \tag{A 2}$$

with only one half the contribution of $W = \pm M$ included in the sum. These transformations can be handled efficiently by the fast-Fourier-Transform algorithm (see Cooley & Tukey 1965). The above transformations then approximate $\partial f_0/\partial t^+$ and $\partial^3 f_0/\partial t^{+3}$ by $F^{-1}\{\mathrm{i}\pi W F\{f_0\}$ and $-F^{-1}\{\mathrm{i}\pi^3 W^3 F\{f_0\}\}$. With a central-difference approximation for $\partial f_0/\partial\tau$ the numerical scheme to solve (4.3) is then given by

$$[f_0(t^+, \tau+\Delta\tau) - f_0(t^+, \tau-\Delta\tau)] = \left[3\mathrm{i} f_0\,\Delta\tau - 2\mathrm{i}\frac{\bar{A}}{\epsilon}\Delta\tau\right] F^{-1}\{\pi W F\{f_0\}\}$$

$$-\frac{\delta^2}{3\epsilon}\mathrm{i}\,\Delta\tau\,F^{-1}\{\pi^3 W^3 F\{f_0\}\} + \frac{\pi\omega}{\epsilon}(1-\cos 2\pi\omega)\sin\pi t^+. \tag{A 3}$$

The practical implementation of (A 3) is discussed in a technical report by Copeland (1977). The same basic approximation scheme is then used for (5.1) and (5.3). The inclusion of the damping term in (5.3) is straightforward. The evaluation of the convolution integral in (5.1) involves the inclusion of an additional fast Fourier transform. In discrete Fourier space the integral in (5.1) can be expressed as

$$\tfrac{1}{4}\beta[\tfrac{1}{2}\pi W|^{\frac{1}{2}}(1 + \mathrm{i}\,\mathrm{sgn}\,W)\,F\{f_0\}, \tag{A 4}$$

where $F$ is given by (A 1), and in physical space as

$$F^{-1}\{\tfrac{1}{4}\beta[\tfrac{1}{2}\pi W|^{\frac{1}{2}}(1 + \mathrm{i}\,\mathrm{sgn}\,W)\,F\{f_0\}\}, \tag{A 5}$$

where $F^{-1}$ is given by (A 2).

Then the numerical scheme (A 3) is readily adapted to include the contribution

from the additional integral term in (5.1). Due to the expense of high-accuracy, long-time, numerical computation, the solution profiles are intended only for graphical display. Most of the calculations were carried out with a mesh size $\Delta t^+ = 0.03125$ and a time step $\Delta\tau = 5.21 \times 10^{-4}$.

As discussed in Fornberg & Whitham (1978) the leapfrog time-differencing scheme (A 3) may under certain circumstances be subject to separation instabilities between two successive time levels. To avoid separation, as suggested by Fornberg & Whitham, the solution was averaged, every 40 time steps, over adjacent time levels and then the scheme restarted with the new averaged values. A further source of separation occurs when every second mesh point separates from every other second value for a given $\tau$. To avoid this the appropriate frequency component corresponding to the separation of every second mesh point was monitored throughout the computation and removed when irregularities were detected. Checks were also made to ensure that such irregularities were numerical in origin.

## REFERENCES


Betchov, R. 1958 Nonlinear oscillations of a column of gas. *Phys. Fluids* **1**, 205–212.

Chester, W. 1964 Resonant oscillations in closed tubes. *J. Fluid Mech.* **18**, 44–64.

Chester, W. 1968 Resonant oscillations of water waves I. Theory. *Proc. R. Soc. Lond.* A **306**, 5–22.

Chester, W. & Bones, J. A. 1968 Resonant oscillations of water waves II. Experiment. *Proc. R. Soc. Lond.* A **306**, 23–39.

Chirikov, B. V. 1979 A universal instability of many dimensional oscillator systems. *Physics Rep.* **52**, 263–379.

Cooley, J. W. & Tukey, J. W. 1965 An algorithm for the machine computation of complex Fourier series. *Math. Comp.* **19**, 297–301.

Copeland, B. 1977 A description of a Fourier method for Korteweg–de Vries type equations. *Tech. Rep.* 77-2, Department of Mathematics, University of British Columbia.

Cox, E. A. & Mortell, M. P. 1983 The evolution of resonant oscillations in closed tubes. *Z. angew. Math. Phys.* **34**, 845–866.

Fermi, E., Pasta, J. R. & Ulam, S. M. 1955 Studies of nonlinear problems. In *Collected Papers of Enrico Fermi*, vol. 2, pp. 978–988. University of Chicago Press, Chicago, Illinois.

Fornberg, B. 1975 On a Fourier method for the integration of hyperbolic functions. *SIAM J. Numer. Anal.* **12**, 504–528.

Fornberg, B. & Whitham, G. B. 1978 A numerical and theoretical study of certain nonlinear wave phenomena. *Phil. Trans. R. Soc. Lond.* A **289**, 373–404.

Jones, A. F. & Hulme, A. 1983 The hydrodynamics of water on deck. Contributed paper at 25th British Theoretical Mechanics Colloquium (unpublished).

Kevorkian, J. & Cole, J. D. 1981 *Perturbation Methods in Applied Mathematics.* Springer.

Kreiss, H. O. & Oliger, J. 1972 Comparison of accurate methods for the integration of hyperbolic equations. *Tellus* **24**, 199–215.

Lettau, E. 1939 Messungen an Gasschwingungen grosser Amplitude in Rohrleitungen. *Deutsche Kraftfahrforsch.* **39**, 1–17.

Miles, J. 1976 Korteweg–de Vries equation modified by viscosity. *Phys. Fluids* **19**, 1063.

Mortell, M. P. 1977 The evolution of nonlinear standing waves in bounded media. *Z. angew. Math. Phys.* **28**, 33–46.

Mortell, M. P. & Seymour, B. R. 1980 A simple approximate determination of the stochastic transition for the standard mapping. *J. Math. Phys.* **21**, 2121–2123.

Ockendon, J. R. & Ockendon, H. 1973 Resonant surface waves. *J. Fluid Mech.* **59**, 397–413.

Ott, E. & Sudan, R. N. 1970 Damping of solitary waves. *Phys. Fluids* **13**, 1432–1434.

SEYMOUR, B. R. & MORTELL, M. P. 1973 Resonant acoustic oscillations with damping: small rate theory. *J. Fluid Mech.* **58**, 353–373.

SEYMOUR, B. R. & MORTELL, M. P. 1980 A finite rate theory of resonance in a closed tube: discontinuous solutions of a functional equation. *J. Fluid Mech.* **99**, 365–382.

SEYMOUR, B. R. & MORTELL, M. P. 1985 The evolution of a finite rate periodic oscillation. *Wave Motion* **7**, 399–409.

VERHAGEN, J. H. G. & VAN WIJNGAARDEN, L. 1965 Nonlinear oscillations of fluid in a container. *J. Fluid Mech.* **22**, 737–752.

YUEN, H. C. & FERGUSON, W. E. 1978*a* Relationship between Benjamin–Feir instability and recurrence in the nonlinear Schrödinger equation. *Phys. Fluids* **21**, 1275–1278.

YUEN, H. C. & FERGUSON, W. E. 1978*b* Fermi–Pasta–Ulam recurrence in the two-space dimensional nonlinear Schrödinger equation. *Phys. Fluids* **21**, 2116–2118.

ZABUSKY, N. J. & KRUSKAL, M. D. 1965 Interaction of 'solitons' in a collisionless plasma and the recurrence of initial states. *Phys. Rev. Lett.* **15**, 240–243.